Electronic and magnetic properties of single vacancy graphene with hydrogen adsorptions analyzed using density functional theory method

Electronic and magnetic properties of single vacancy graphene with hydrogen adsorptions analyzed using density functional theory method

Maya Mahirotul Septya[1, a], Retno Asih[1], Rizal Arifin[2], Darminto[1, b]

[1] Department of Physics, Faculty of Science and Data Analytics, Institut Teknologi Sepuluh Nopember, Surabaya 60111, Indonesia
[2] Department of Mechanical Engineering, Faculty of Engineering, Universitas Muhammadiyah Ponorogo, 63471, Indonesia

E-mail: [a]mayamahirotul1@gmail.com, [b]darminto@physics.its.ac.id

Abstract. Graphene has become an exciting material to be studied because of its unique properties. One of the interesting phenomena is the change of its electronic and magnetic properties due to impurities adsorption. By using the spin-polarized density functional theory (DFT) method, we simulate single vacancy graphene with the adsorption of hydrogen atoms around the dangling bond to determine the electronic and magnetic properties of the material. In this study, we use a 4×4×1 supercell of single-layered graphene. We have four models, i.e., single vacancy graphene, and graphene with hydrogen adsorption in the dangling bond site with the atom's variation number (H = 1, 2, 3 atoms). Our results show that the modifications of graphene in the form of single vacancy and hydrogen adsorptions makes the graphene material metal, except for the SV+2H model which shows a semiconductor characteristic. The presence of a single vacancy affects the magnetic moment of the modeled graphene layer. A single vacancy on the modeled graphene layer results in a total magnetic moment of 0.69 μ_B/cell. In the single vacancy graphene with three hydrogen atoms adsorption, we acquire the total magnetic moment of 0.15 μ_B/cell. This study shows that defects in the forms of vacancies and adsorption of hydrogen atoms can initiate magnetism on graphene. These results open a way of using graphene to create nanomagnetic devices.

1. Introduction

Graphene two-dimensional material is still fascinating since its discovery [1]. Two-dimensional (2D) structure makes graphene the building block of other carbon-based materials such as graphite, CNT, and fullerenes, depending on how it is arranged. Pristine graphene is composed of carbon atoms and forms a hexagonal lattice structure. With only a few atoms of thickness, graphene has the advantages of being thin, light, transparent, and flexible in terms of mechanical properties [2], [3]. Besides, this material also has advantages in various scopes, including high carrier mobility (~2×10^5 cm^2/V s) [4], low electrical resistivity (~10^{-6} Ωm) [5], high thermal conductivity (~5.30×10^3 W/mK) [6], and optical transparency up to 97.7% [7]. In nature, pristine graphene undergoes sp^2 hybridization with the valence and conduction bands touching each other at the Dirac point, so it has zero band gaps [8]. Besides, ideal graphene is known as non-magnetic material [9]. Therefore, pristine graphene becomes inapplicable materials.

Until now, several methods have been known to modify the bandgap structure and magnetism of graphene to make it more applicable, including functionalization, giving of defects [10] (ex: vacancies),

impurities (AEM [11], Na [12], and Boron [13]), and edge effects [14]. Based on experimental research conducted by Ristiani et al., by only inserting Na atoms, the magnetic properties of rGO can be increased [12]. Pure graphene has strong diamagnetism properties [15]. However, when the graphene is given a defect in the form of a single vacancy, the magnetism changes to paramagnetism. The magnetic moment of graphene ranges from 1.12-1.53 μ_B per vacancy depending on the defect concentration [16]. Furthermore, the adsorption of one H atom could induce a spin moment of $1\mu_B$ because the binding of one H atom could give rise to a saturated one p_z bond [10]. Additionally, when all the atoms in the graphene unit cell experienced functionalization with H atoms, there would be a transition of electronic properties from metal to insulator [17].

The binding of the H atom is very likely because the formation of a vacancy will create a dangling bond at the three closest carbon atoms to the vacancy site. The dangling bond is very reactive to the presence of other atoms, such as the H atom. Such a configuration will undoubtedly affect the electronic and magnetic properties of graphene. Therefore, we will conduct a study related to the effect of the binding of H atoms on C atoms near the vacancy sites on the electronic and magnetic properties of graphene as the host material. To better understand the interactions between electrons in the system, we calculate using the Density Functional Theory (DFT) method so that the results obtained will be close to the actual conditions.

2. Methods

All atomic calculations were carried out using Quantum-ESPRESSO packages code based on the spin–polarized Density Functional Theory (DFT) method. We performed the first-principle Projector Augmented-Wave (PAW) pseudopotentials calculations based on DFT. The type Pardew – Burke – Ernzernof (PBE) of Generalized Gradient Approximation (GGA) to functionalize exchange-correlation potential is used in this DFT calculation. The plane-wave cut-off energy was 952 eV following convergence study results. We computed a system of 4×4 supercells graphene with 32 number of atoms for pristine graphene. Also, for a single vacancy model of graphene, we removed one carbon atom from supercells. Besides, we also modeled adsorption H atoms on graphene supercells. The geometry optimization uses Brillouin zone sampling of 6×6×1 k-points with the centre in Γ point based on converged study results and the research before [18]. The self–consistent field (SCF) calculation was performed with 12×12×1 k-points, and the non–self-consistent field (NSCF) with 16×16×1 k-points was used for DOS calculation. There were four simulated models, i.e., single vacancy graphene, and hydrogen adsorption in the dangling bond site with the variation number of the atom (H=1, 2, 3 atoms). Graphene was vacuumed by 20 Å of distance aimed to isolate that system.

3. Results and discussion

From graphene supercells of 4×4×1, we take out a C atom from the pristine graphene and optimize that model, as we can see in Figure 1(a) to (d). According to the optimized geometry of single vacancy (SV), we obtain the planar configuration similar to pristine graphene, which showed the average C-C bond length is 1.4188 Å as in the previous report [19]. For the second model, the interesting one, SV has then adsorbed an H atom (SV+1H) illustrated in Figure 1(b). Blue and red colour indicate the carbon and hydrogen atoms, respectively. The existing one is the emergence of distortion that causes the distance of C1-C2 ≠ C2-C3 ≠ C1-C3, as shown in Table 1. Optimized result of structure exhibits rather than wrinkle [20]. From that figure, we can reveal that the existence of the H atom will change the planar surface of graphene. The position of a C atom is slightly up due to the binding of an H atom, and a few of the C atoms are slightly down because of the rising effect. The rise of C1 is 0.7527 Å over the plane. Consequently, the position of C2 and C3 are down compared to the initial one. As we know that the length of the C-H bond and the average length of the C-C bond is 1.0781 Å and 1.4256 Å, respectively. For details, see Table 1.

A hydrogen atom is then adsorbed again on the C2 atom, so the third model has been obtained, as shown in Figure 1(c). It is seen that the surface of SV+2H is still wrinkling as before. We acquire the mean length of the C-C bond decreases slightly from before, i.e., 1.4253 Å. As the previous explanation,

the optimized structure has a slightly up and down of carbon atoms from the graphene plane. The atomic distance of C-H for both is 1.0725 Å, and the height of H atoms to the basis plane of graphene can be seen in Table 1. The position of atoms C1, C2, H1, and H2 shows symmetry.

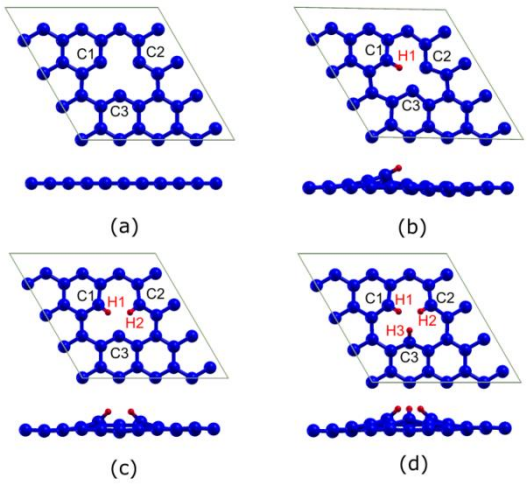

Figure 1. The optimized structure of (a) SV model (b) SV+1H model (c) SV+2H model (d) SV+3H model. Blue indicates carbon atom and red indicates hydrogen atom.

For the last model, some atoms including carbon and hydrogen located over the basis plane of graphene, also have the wrinkle condition [20]. More details can be seen in Table 1. The more adsorption of H atoms, the smaller the distance between C-H that we get. The four models' optimized geometry can change the initial lattice parameters, as shown in Table 2. All models except SV+2H show similar lattice parameters (a = b). The exception model indicates the asymmetry of crystal cells.

Table 1. The obtained structure parameters of geometry optimization. $\underline{d}$ is the average distances, d is the atomic distances and h is the heights of atoms from the graphene planar surface.

Model	$\underline{d}_{C\text{-}C}$ (Å)	$d_{C\text{-}H}$ (Å)	h_{C1} (Å)	h_{C2} (Å)	h_{C3} (Å)	h_{H1} (Å)	h_{H2} (Å)	h_{H3} (Å)
SV	1.419 ± 0.015	-	0.0033	0.0033	0.0033	-	-	-
SV+1H	1.426 ± 0.032	1.0781	0.7527	-0.0731	-0.0731	1.2136	-	-
SV+2H	1.425 ± 0.011	1.0725	0.4972	0.4972	-0.1672	1.1744	1.1744	-
SV+3H	1.428 ± 0.014	1.0587	0.5603	0.5603	0.5603	1.2404	1.2404	1.2404

Table 2. Lattice parameters of optimized geometry

Model	Lattice Parameters (Å)		
	a	b	c
SV	9.8406	9.8406	20
SV+1H	9.8777	9.8777	20
SV+2H	9.9367	9.8498	20
SV+3H	9.9138	9.9138	20

Figure 2(a) shows the band structure calculation result of the SV model. We can observe that the Fermi level through the valence band indicates a transition of semimetal electronic properties to metal [21]. This model has p-type conductivity due to the electron deficiency system. Next, we find an energy gap opening, as shown in Table 3, which is due to the broken symmetry in the graphene sublattice [22].

Figure 2(a) also shows the presence of two bands with a high degree of splitting around the Fermi energy [15]. It is predicted that the appearance of these bands can initiate magnetic order [21].

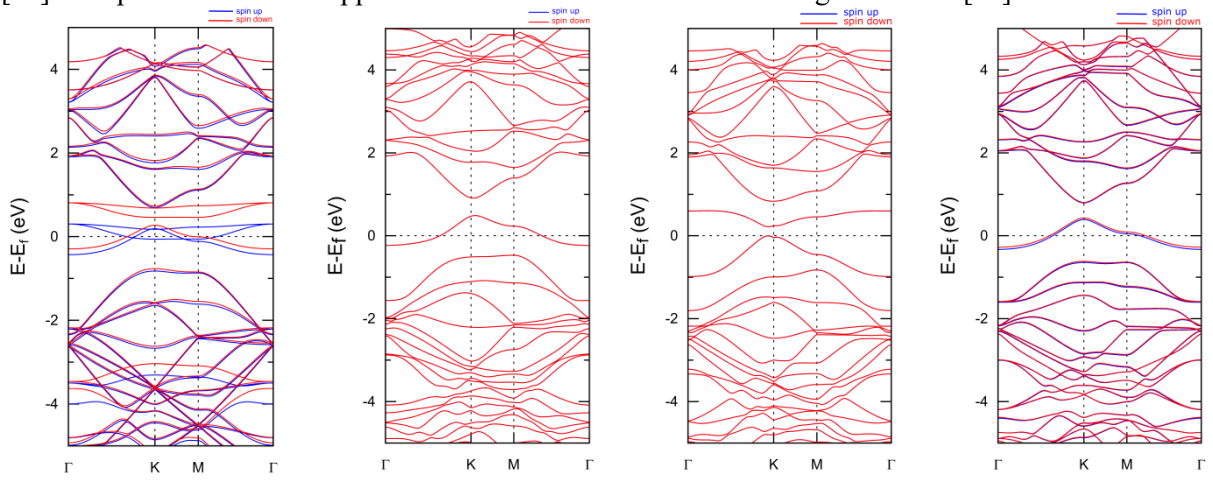

(a) (b) (c) (d)

Figure 2. Band structure of (a) SV model (b) SV+1H model (c) SV+2H model (d) SV+3H model

The SV+1H model has the same tendency as the SV model where the Fermi level through the valence band so that this model is metallic [21] (see Figure 2(b)). From Table 3, we know that the energy gap opening is smaller than the SV. This model has a significant difference from the previous model in the formation of splitting bands. The band structure of up and down states stack at the same point. The adsorption two hydrogen atoms (SV+2H model) also have the same tendency as the previous model, which have stacking bands of up and down states. The Fermi level is at the maximum point of the valence band (see Figure 2(c)), so this model is a semiconductor. The last model, SV+3H, has the same behaviour with two former models (SV and SV+1H), in which the Fermi level through the valence bands (see Figure 2(d)). Furthermore, we find a tiny splitting band which is predicted to give rise to the magnetic properties in this model [15].

Table 3. The summary of electronic and magnetic properties within the energy gap and the magnetic moment of the calculation models

Model	E_g (eV)		Magnetic Moment (μ_B)
	up	down	
SV	0.5198	0.4093	0.69
SV+1H	0.4190	0.4190	0.00
SV+2H	0.2957	0.2932	0.00
SV+3H	0.4015	0.3740	0.15

Based on the SPDOS calculation results, the SV model is not symmetrical between DOS spin up and DOS spin down, as shown in Figure 3(a). These results indicate a transition in the magnetic properties of the model [21]. The total magnetic moment for this model is 0.69 μB/cell. The magnetic moment is focused on the three carbon atoms near the vacancy site. Each carbon atom contributes a magnetic moment of 0.0754 μB. The formation of a single vacancy in graphene will cause the four unpaired electrons to spread over the three carbon atoms near the vacancy site. Since the magnetic moments produced by the three carbon atoms are of the same value, it is assumed that only the unpaired electrons in the molecular orbital σ contribute to the transition to magnetism.

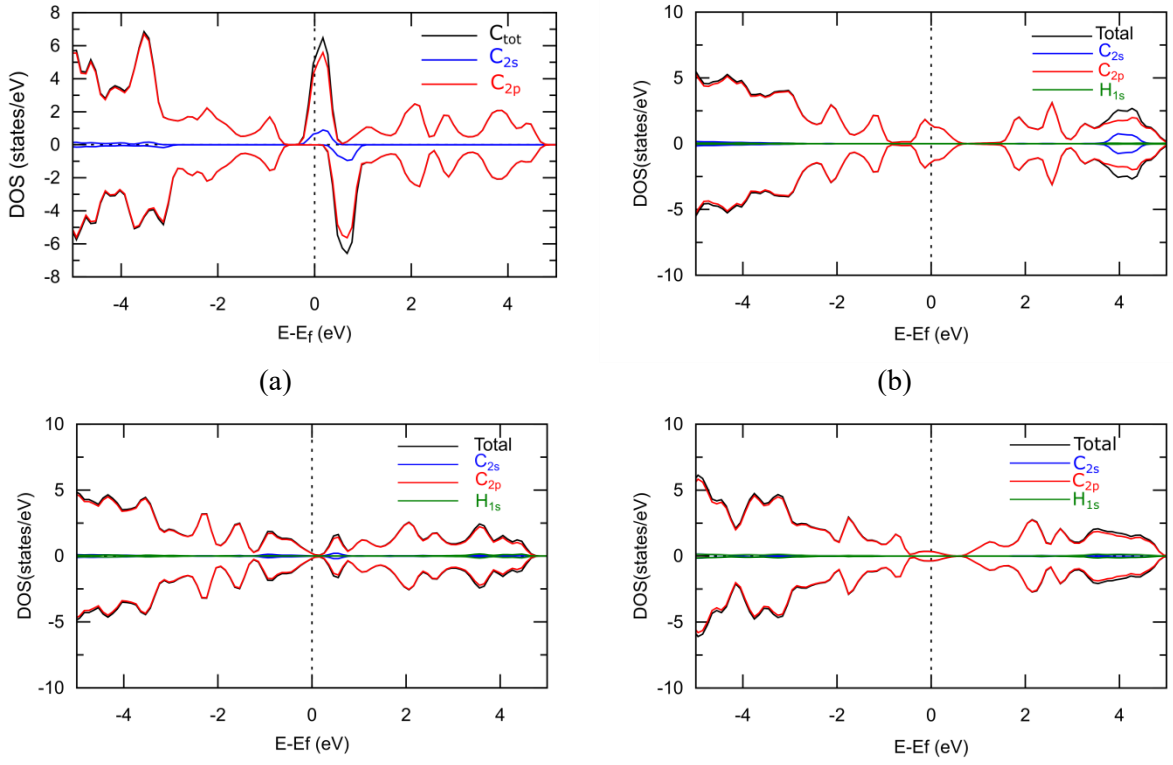

Figure 3. SPDOS of (a) SV model (b) SV+1H model (c) SV+2H model (d) SV+3H model

The SPDOS calculation results for the SV+1H model are shown in Figure 3(b). These results indicate a symmetrical feature between the DOS of spin up and spin down. This condition suggests that this model has non-magnetic properties. This situation can be understood by the appearance of the distortion, as described in the structural analysis section. The distortion is formed as a result of the interaction between the unpaired electrons held by two carbon atoms, which are the closest neighbours of the vacancy site. With this interaction, the number of unpaired electrons is reduced. The binding of H atoms depletes the number of unpaired electrons, which has the potential to induce a magnetic transition, so this model signifies a non-magnetic feature.

The third model (SV+2H) also has a symmetrical DOS between the spin up and spin down as the SPDOS of the second model (see Figure 3(c)), indicates a non-magnetic characteristic. No dangling bond in this model. We assume that H atoms' binding omits the dangling bonds, and the other electron is used together or denoted as coordination covalent bond. Similar to the second model, this model is categorized as non-magnetic. The last model shows the SPDOS illustration of the SV+3H model, as shown in Figure 3(d). A few asymmetrical DOS of spin up and spin down around the dashed line exist when we look detailed. Although the asymmetry is small, it affects the total magnetic moment of 0.15 μB/cell.

To validate our results, we compared the magnetic moments obtained in this study with some previous studies. Goudarzi et al., 2019 reported the magnetic moment in the SV model is 0.89 μB [23]. A slight difference with our results was indicated because they used smaller cut-off energy of 340 eV. This cut-off energy is too small for a system with 4×4×1 supercells, and we have conducted a convergence study to find the optimum cut-off energy value that is 952 eV. Gao et al., 2017 also reported the magnetic state in the SV model with a magnetic moment of 1.5 μB [24]. However, they used different supercell sizes with our models. However, these results validated that the SV model has a magnetic state. Furthermore, for another model SV + xH (x = 1,2,3), we have not found a reference that calculates

the magnetic moment of this model. However, because we used the same simulation parameters as the SV model, the calculated magnetic moment for the SV + xH model (x = 1,2,3) is still acceptable.

4. Conclusions

The effect of a single vacancy (SV) with hydrogen adsorption was investigated by density functional theory (DFT). We have performed calculations on the structure, electronic, and magnetic properties of the models, SV, SV+1H, SV+2H, and SV+3H. Based on the structural analysis, it can be said that the presence of a single vacancy still makes the graphene surface planar. But the adsorption of hydrogen atoms will cause the graphene surface wrinkles [20]. Meanwhile, in terms of electronic properties, we know that all models are metal except SV+2H which shows a semiconductor characteristic. Both the SV and SV+3H models show the presence of splitting bands indicating the appearance of a magnetic moment [15] which is then proven by the obtained magnetic moment of 0.69 and 0.15 μ_B, respectively.

Acknowledgement

This research was partially supported by PDUPT Research Grant No: 186/PKS/ITS/2020, ITS – Kemenristek/BRIN, 2019 – 2020.

References

[1] K. S. Novoselov *et al.* 2005 *Nature* **438** 197-200
[2] D. Akinwande *et al.* 2017 *Extreme Mechanics Letters* **13** 42–77
[3] A. Armano and S. Agnello 2019 *C* **5** 67
[4] D. De Fazio *et al.* 2019 *ACS Nano* **13** 8926–35
[5] S. Ren, P. Rong, and Q. Yu 2018 *Ceramics International* **44** 11940–55
[6] A. A. Balandin *et al.* 2008 *Nano Lett.* **8** 902–7
[7] Y. Ma and L. Zhi 2019 *Small Methods* **3** 1800199
[8] O. V. Kibis, K. Dini, I. V. Iorsh, and I. A. Shelykh 2017 *Phys. Rev. B* **95** 125401
[9] S. Nigar, Z. Zhou, H. Wang, and M. Imtiaz 2017 *RSC Advances* **7** 51546–80
[10] E. J. G. Santos, A. Ayuela, and D. Sánchez-Portal 2012 *New J. Phys.* **14** 043022
[11] M. Sun *et al.* 2015 *Applied Surface Science* **356** 668–73
[12] Ristiani, D., Asih, R., Puspitasari, N. S., Baqiya, M. A., Kato, M., Koike, Y., ... & Furukawa, Y. 2020 *IEEE Transactions on Magnetics* **56**
[13] T. Wu, H. Shen, L. Sun, B. Cheng, B. Liu, and J. Shen 2012 *New J. Chem.* **36** 1385–91
[14] A. Jabar and R. Masrour 2020 *Chinese Journal of Physics* **64** 1-8
[15] Y. Zhang *et al.* 2016 *Phys. Rev. Lett.* **117** 166801
[16] O. V. Yazyev and L. Helm 2007 *Phys. Rev. B* **75** 125408
[17] J. Zhou, Q. Wang, Q. Sun, and P. Jena 2010 *Phys. Rev. B* **81** 085442
[18] S. Casolo, O. M. Løvvik, R. Martinazzo, and G. F. Tantardini 2009 *J. Chem. Phys.* **130** 054704
[19] Q. Zhou, Y. Yong, W. Ju, X. Su, and X. Li 2017 *Physica E: Low-dimensional Systems and Nanostructures* **91** 65–71
[20] D. W. Boukhvalov, M. I. Katsnelson, and A. I. Lichtenstein 2008 *Phys. Rev. B* **77** 035427
[21] M. Ali, X. Pi, Y. Liu, and D. Yang 2017 *AIP Advances* **7** 045308
[22] R. Skomski, P. A. Dowben, M. S. Driver, and J. A. Kelber 2014 *Materials Horizons* **1** 563–71
[23] M. Goudarzi, S. S. Parhizgar, and J. Beheshtian 2019 *Opto-Electronics Review* **27** 130–6
[24] F. Gao and S. Gao 2017 *Scientific Report* **7** 1792